# Mimecan Regulates Corticosterone Secretion and Plays A Critical Role in Adrenal Responses to Stress

**Bin Su**
Shanghai Tenth People's Hospital
**Qianyue Zhang**
Shanghai 9th Peoples Hospital Affiliated to Shanghai Jiaotong University School of Medicine
**Xuesong Li**
Minhang Hospital, Fudan University
**Huimin Yu**
Shanghai 9th Peoples Hospital Affiliated to Shanghai Jiaotong University School of Medicine
**Ping Li**
Shanghai 9th Peoples Hospital Affiliated to Shanghai Jiaotong University School of Medicine
**Junhua Ma**
Shanghai 9th Peoples Hospital Affiliated to Shanghai Jiaotong University School of Medicine
**Huangming Cao**
Shanghai 9th Peoples Hospital Affiliated to Shanghai Jiaotong University School of Medicine
**Fei Sun**
Shanghai 9th Peoples Hospital Affiliated to Shanghai Jiaotong University School of Medicine
**Shuangxia Zhao**
Shanghai 9th Peoples Hospital Affiliated to Shanghai Jiaotong University School of Medicine
**Cuixia Zheng**
Anhui Provincial Hospital
**Ying Ru**
Icahn School of Medicine at Mount Sinai
**Huaidong Song** ( huaidong_s1966@163.com )
Shanghai 9th Peoples Hospital Affiliated to Shanghai Jiaotong University School of Medicine
https://orcid.org/0000-0003-2030-8179

---

**Research**

**Keywords:** Mimecan, Stress response, Hypothalamic-pituitary-adrenal axis, Adrenal gland

**Posted Date:** September 17th, 2020

**DOI:** https://doi.org/10.21203/rs.3.rs-72858/v1

# Abstract

**Background:** A functional hypothalamic-pituitary-adrenal (HPA) axis is critical for host defenses to outside stimuli. The adrenal cortex is seemingly endowed with distinct functional units that are regulated by adrenocorticotropic hormone (ACTH). We have found that mimecan, a small leucine-rich proteoglycan expressed in the adrenal gland, has yet to be characterized in functional terms.

**Results:** Herein, we have demonstrated the following properties: 1) adrenal mimecan expression in mouse models is significantly downregulated under hypoglycemia and scalded stress; 2) expression of mimecan in adrenal cells may be downregulated through ACTH or upregulated by glucocorticoid via related receptors (GRs); and 3) mimecan stimulates corticosterone secretion in adrenal tissues. The latter was proven using *in vivo* and *in vitro* studies to confirm the ACTH-independent activity of mimecan-maltose-binding protein (-MBP). Relative to litter-mate mice, the basal-state diurnal rhythm of corticosterone secretion is disrupted in mimecan knockout mice, and corticosterone secretion is increased under restraint stress conditions.

**Conclusions:** These findings offer the first evidence that mimecan is key in regulating the HPA axis, assuming a critical role in adrenal responses to stress.


# Background

Each organism must maintain a complex dynamic equilibrium, otherwise known as homeostasis. Stress is a state in which homeostasis is threatened by emotional or physical stressors, although various physiologic and behavioral adaptive responses may be restorative in this regard(1). Exposure to stressful challenges incites behavioral and physical changes that are normally adaptive and limited over time, improving chances for survival. These responses must be appropriate in magnitude and duration; otherwise, they may have detrimental effects on numerous physiologic functions of organism, leading to a state of disease-causing disturbed homeostasis.

The HPA axis is pivotal in responses to stress. The HPA axis activation is initiated by the activation of parvocellular neurons in the paraventricular nucleus (PVN) of the hypothalamus and the release of corticotropin-releasing hormone (CRH) and arginine vasopressin (AVP) from the external zone of the median eminence into portal circulation(2, 3). CRH acts upon anterior pituitary, stimulating synthesis and secretion of adrenocorticotropic hormone (ACTH), which then stimulates adrenal cortex to secrete glucocorticoid (GC) (cortisol in humans; corticosterone in rodents)(2, 3). A primary effect of stress-induced glucocorticoid release is the inhibition of ongoing HPA-axis activation through negative feedback at the level of hypothalamus and pituitary and at upstream limbic structures, thus inhibiting ACTH and CRH secretion through mineralocorticoid (MR) and glucocorticoid receptors (GR)(2, 3).

HPA-axis dysfunction is implicated in the pathogenesis of various stress-related physical and psychological diseases, such as Cushing' syndrome, panic disorder, and post-traumatic stress disorder, all of which reflect heightened HPA-axis activity. On the other hand, adrenal insufficiency, chronic fatigue

syndrome, and atypical depression are associated with reduced activity of the HPA axis(4, 5). Hence, mechanisms regulating functions of the HPA axis are of utmost importance in managing stress-related disease. Such mechanisms unfortunately have yet to be fully clarified.

Originally isolated from bone, mimecan (osteoglycin) belongs to the family of small leucine-rich proteoglycans (SLRPs)(6). SLRPs are abundant in bone matrix, cartilage cells, and connective tissues. They are also essential for collagen fibrillogenesis and are central to cellular growth, differentiation, and migration(7). Although the mimecan gene encodes a 34-kDa full-length protein, a 12-kDa mature protein corresponding to the 105 carboxyl-terminal amino acids of mimecan has been isolated from bovine bone. A 25-kDa keratan sulfate glycoprotein corresponding to the 223 carboxyl-terminal amino acids of mimecan has been isolated from bovine cornea(8).

To date, the physiologic functions of mimecan remain obscure. We have previously cloned the full-length cDNA of human mimecan (accession number: AF100758)(9), establishing mimecan as a novel satiety hormone in adipose tissue propagated by IL-1β and IL-6 induction within hypothalamus(10). Our previous studies have also shown that mimecan is expressed in human pituitary corticotroph cells and the AtT-20 mouse corticotroph cell line and mimecan gene expression in pituitary corticotroph cells is up-regulated by glucocorticoid (GC) in a time- and dose-dependent manner(9, 11). Besides, mimecan stimulated adrenocorticotrophic hormone (ACTH) secretion in pituitary corticotroph AtT-20 cells(12). Because mimecan is important in the functions of HPA axis, the present study was undertaken to further explore the expression of mimecan in adrenal glands and its effects on HPA axis functions.

# Materials And Methods

### *Animals*

Wild-type C57BL/6 mice were bought from Shanghai Experimental Animal Center, Chinese Academy of Sciences. Mimecan knockout mice ($mim^{-/-}$) were generated as described elsewhere(11, 12). The animals were housed in a temperature-controlled room (23º C) subject to12-h light/dark cycles, allowing *ad libitum* access to chow and water. Adult male (8-10 week-old) $mim^{-/-}$ mice and age-matched wild-type C57BL/6 mice were used for experiments. All animal-related investigations were conducted in accordance with our institutional guidelines on ethical animal care and were approved by the Animal Care and Use Committee in the Ninth Hospital Affiliated to Shanghai Jiaotong University School of Medicine.

### *Hypoglycemic-mouse model*

C57BL/6 mice were randomly assigned to stressed or control group of each time point 0h, 1h, 2h, 4h, 6h, 8h, and 12h (10 mice for each time point). C57BL/6 mice of stressed group were fasted overnight for 12 h. Blood glucose levels of 0h were assayed in blood obtained by tail cuts at 8 am using a glucometer (Accu-Chek Compact; Roche Diagnostics), and intraperitoneal (IP) injections of insulin (3 IU/kg) were delivered at 9 am(13). The mice were subsequently sacrificed by cervical dislocation after blood glucose measure in tail vein at 1h, 2h, 4h, 6h, 8h and 12h after injection and adrenal glands and lung tissues were

immediately taken and frozen at -80 ºC. The target blood glucose concentration was <40 mg/dl, a value conventionally used to define hypoglycemia during development. The other half of the litter was injected with the equivalent volume of 0.9% saline (control group).

### *Scalded-mouse model*

C57BL/6 mice were randomly assigned to scalded or control group (15 mice per group) 24 hours after the hairs of mice were removed by using hair removal agents made of barium sulfide, mice were randomly divided into stressed group and control group. Both groups of mice were anesthetized with 2.5% pentobarbital sodium at the dose of 35mg/kg and placed on boards designed for 10% of total body surface area exposure and immersed (8 seconds) in a water bath held at 90°C (stress group) or room temperature (control group)(14). This method delivers a full-thickness cutaneous burn as confirmed by histological examination. Four hours after burn or sham injury, the mice were fully recovered from anesthesia and were sacrificed by cervical dislocation. Portions of scalded skin and unilateral were fixed in buffered formalin for morphologic evaluation. Part samples of adrenal glands and lung tissues were formalin-fixed and paraffin-embedded and part were immediately frozen and stored at -80°C until analyzed.

### *Restraint stress model*

5 $mim^{-/-}$ mice and 5 wild-type litter mates were restrained using plastic tubes with a narrow end that exposed the mouse's head, obtaining blood (by tail cuts) after 60 min of restraint and being released for 60 min.

### *ACTH stimulation test*

C57BL/6 mice were randomly assigned to each group (12 mice for each time point). We administered ACTH (0.085 IU/g body weight) in mice by IP injection (9:00 am), then sacrificing the mice by cervical dislocation at the indicated time points 0h, 2h, 4h, 6h, 8h, and 12h. Adrenal glands were immediately taken and frozen at -80. ACTH (sigma) were diluted by sterile 0.9% saline and placed on ice to remain effective. Corresponding control groups were stimulated using equivalent volume of 0.9% saline. In $mim^{-/-}$ mice and wild-type litter mates (21 $mim^{-/-}$ mice and 15 WT mice), same dose of ACTH was given by IP injection at 9am. Blood samples for corticosterone measurement were removed from the tail vein before and 15min, 30min, 45min, 60min, and 120min after ACTH administration.

### *Dexamethasone suppression test*

C57BL/6 mice were randomly assigned to each group (10 mice per group for each time point). Dexamethasone (DEX, sigma, 0.05 ug/g body weight) or 0.9% saline were administered by intramuscular (IM) injection, mice were sacrificed by cervical dislocation at the indicated time points 2h, 12h and 36h at 7:30pm (when cortisol secretion peaks) and adrenal glands were immediately taken and frozen at -80. In $mim^{-/-}$ mice and wild-type litter mates (21 $mim^{-/-}$ and 15 WT ), same dose of DEX was given by IM

injection. Blood samples for corticosterone and ACTH measurement were removed from the tail vein 5h, 8h, 24h and 32h after DEX administration at 12am.

### *Circadian rhythm determination of corticosterone*

11 $mim^{-/-}$ mice and 12 wild-type litter mates were used, and blood was taken from tail vein every 4 h for serial serum corticosterone determinations.

### *Mimecan-MBP stimulation*

C57BL/6 mice were administered with 0.1 μmol/kg mimecan-MBP, 0.1 μmol/kg MBP, or an equivalent volume of 0.9% saline by IP injection at 9am. Mice were sacrificed by decapitation and trunk blood was obtained 0.5h, 2h, 24h and 48h after injection for hormonal analysis. For 24h and 48h group, injection was repeated every 8 hours.

### *Primary adrenal gland cell isolation and cell culture*

Primary adrenal gland cells were isolated by collagenase digestion method. Adrenal glands were obtained from 20 adult male C57BL/6 mice after decapitation. Tissues were washed with HBSS. Pieced sliced fragments were dispersed in preparation buffer containing 30mg/ml type 1 collagenase (Sigma). Dispersed cells were centrifuged and resuspended in F-12K medium containing 15% horse serum and 2.5% fetal calf serum. Then, cells were distributed in 12-well plates and incubated at 37°C under 5% CO2 for 12 h until they were used.

The Y-1 mouse adrenocortical tumor cell line was obtained from American Tissue Type Collection (ATCC, VA, USA), which is a subclone of the corticotropin-responsive cell line originally developed by Yasumura et al.(15). The cell line was maintained in F-12K medium containing 15% horse serum and 2.5% fetal calf serum (FCS) (GIB-CO, USA) in a 5% CO2-humidified atmosphere at 37°C. All cell cultures were routinely passaged at 90–95% confluency. Before the experiment, cells were preincubated with F-12K medium containing 0.2% BSA for24 h. Then treated with ACTH (sigma), DEX (sigma), MBP-mimecan fusion protein made in our lab(10), specific cell pathway inhibitors, and so on. Medium samples were collected and stored at-80◦C at the end of the experiments for hormone content analysis. Cells in the culture plates were processed for RNA extraction as indicated below.

### *Quantitative real-time polymerase chain reaction (PCR)*

Gene expression was assessed by relative quantification ($2^{\Delta\Delta Ct}$ method), using an ABI Prism 7300 Real-Time PCR System (Applied Biosystems, Foster City, CA, USA), 96-well plates, and SYBR Premix Ex Taq (Takara Bio, Shiga, Japan) according to the manufacturer's instructions(16). All samples were normalized to values of β-actin; results were expressed as fold-changes of threshold cycle (CT) values relative to controls. Cycling parameters were 95ºC for 10 s, then 40 cycles of 95ºC for 5 s and 60ºC for 31 s. Analysis was done in quadruplicate, repeating experiments independently three times. Primers were showed in **Supplementary Table 1**.

### *Blood collection and hormone assays*

Whole blood was collected into iced empty or heparinized tubes. Blood was centrifuged at 2000 g for 20 min at 4 ºC, and then plasma or serum were recentrifuged at 6000 g for 10 min at 4 ºC and stored at -80 ºC for subsequent determination of ACTH in plasma and corticosterone in serum. ACTH or corticosterone concentrations of the mouse plasma or serum and Y-1 cell culture media were measured by ELISA commercially available kits (EK-001-21, Phoenix pharmaceuticals, USA and Cayman, USA) as described by the manufacturer.

### *Fusion protein purification and antibody production*

Mimecan-MBP fusion protein and MBP protein purification was conducted as described earlier by our group(10). The cDNA encoding 12 kDa human mimecan (residues 175–279) was subcloned into pGEX-5X-2 (GE Healthcare) and overexpressed in Escherichia coli BL21 (DE3) cells. Purified mimecan-MBP fusion protein was used for antibody production. Rabbits and mice were immunized with recombinant protein in Freund's adjuvant (Sigma-Aldrich, St. Louis, MO, USA) for polyclonal and monoclonal antibody production, respectively. Antibodies were purified using Protein G (GE Healthcare). The monoclonal subtype was identified as IgG1-κ. Human cDNA encoding 12 kDa mimecan (residues 175–279) was subcloned into pMAL-c2x (NEB) and overexpressed in BL21 (DE3) cells. Cells were grown at 37 °C to an optical density at 595nm(A595) of 0.6–0.8, induced with 0.5 mM isopropyl-β-D-thiogalactoside (IPTG) for 5 h, and centrifuged. Cells were sonicated, centrifuged, and the fusion protein in the supernatant was purified by affinity chromatography (MBPTrap HP, GE Healthcare), gel filtration (Superdex 200, 10/300 GL, GE Healthcare), and ion exchange (HiTrap ANX FF, GE Healthcare) chromatography. Purity of the mimecan-MBP fusion protein was 96%, as determined by sodium dodecyl sulfate polyacrylamide gel electrophoresis (SDS-PAGE) and silver staining. MBP was expressed and purified (98%) for use as a control.

### *Northern blot*

Northern blot was performed using the non-isotopic digoxigenin (DIG) Northern Starter Kit (Roche Diagnostics, Rotkreuz, Switzerland) as directed by the manufacturer(17). Target fragments, mouse mimecan, and mouse steroidogenic acute regulatory protein (StAR) were cloned into PGEM-T Easy vectors and confirmed by restriction enzyme digestion and sequence analysis. DIG-labeled probes were generated by transcription, using SP6/T7 RNA polymerase from the DIG RNA Labeling Kit. Total RNA was isolated from mouse tissues by TRIzol reagent (Invitrogen), and spectrophotometry was used to gauge total RNA content. 10 ug mRNA composed of equal amount of mRNA from 10 mice in a group per lane were applied to a 1.2% agarose-formaldehyde denaturing gel and transferred by capillary blotting to positively charged nylon membranes (Roche). The membranes were then baked at 80°C for 2 h. Hybridization was performed at 68°C, with overnight agitation. The membranes were washed twice for 5 min (room temperature), using 2× standard saline citrate (SSC) and 0.1% SDS, then twice for 15 min (68°C) using 0.1× SSC and 0.1% SDS. Finally, the membranes were washed, blocked, and incubated with

anti-DIG serum/alkaline phosphatase conjugate. CDP-Star (Roche) served as the chemiluminescence substrate. Signals were visualized on x-ray film.

### *In situ hybridization*

Target fragments (Mimecan) were cloned into PGEM-T easy vector (Promega) and confirmed by automated sequencing. The RNA probes were labeled by using the DIG or Fluorescein RNA labeling kit (SP6/T7; Roche). The adrenal glands from the C57BL/6 mouse were cut into serial frozen sections (5 um). These sections were first fixed in 4% paraformaldehyde and digested in 1 ug/ml protein kinase buffer. After prehybridization, the sections were incubated with hybridization solution containing 0.5 ng/ul of Fluorescein-labelled probe (for single in situ hybridization) or DIG/ Fluorescein-labelled probes (for double in situ hybridization) in a humidified chamber overnight at 68℃. The post-hybridization slides were washed twice with 2 X SSCT (0.3 M sodium chloride, 30 mM sodium citrate, 0.1% Tween 20)/50% formamide at 68◦C and once with 2X SSCT and 0.2X SSCT at room temperature and then incubated with Anti- Fluorescein AP-conjugate (for single) or anti-DIG-alkaline phosphatase Fab (for double) diluted 1:1000 in blocking solution. After being washed in MABT (0.1 M maleic acid, 0.15 M sodium chloride, 0.1 M Tris-base, 0.1% Tween 20, pH 7.5), they were incubated with staining buffer in a humidified chamber. To terminate the reaction, samples were rinsed several times with nuclease-free water and were visualized by light microscopy.

For double-staining, phenylethanolamine-N methyl transferase (PNMT), tyrosine hydroxylase (TH) or Adrenomedullin (AM) was visualized by phosphatase substrate, BCIP/NBT, according to the protocol used for single-staining, followed by washed twice with MAB (0.1 M maleic acid, 0.15M sodium chloride, 0.1 M Tris-base, pH 7.5) for 20 minutes at room temperature, then incubation with MAB added by 10mM EDTA for 30 minutes at 65℃ to destroy residual anti-DIG-alkaline phosphatase Fab activity.

After blocking for 1 h, sections were incubated overnight at 4℃ with Anti- Fluorescein AP-conjugated secondary antibody, after being washed in MABT, they were incubated with Fast red staining buffer in a humidified chamber. To terminate the reaction, samples were rinsed several times with nuclease-free water and were visualized by light microscopy or fluorescence microscopy（Leica）.

### *Immunohistochemical analysis*

Sections of formalin-fixed, paraffin-embedded adrenal tissue (4-μm thick) of the C57BL/6 mouse were rehydrated. Following microwave antigen retrieval, polyclonal anti-mimecan antibody (1000-fold dilution) was applied for immunostaining, which was generated in our lab by immunizing rabbits with glutathione-S-transferase-mimecan fusion protein, as detailed elsewhere(10). Chromogenic reactions were peroxidase-based, relying on the EnVision+ system (Dako [Agilent], Santa Clara, CA, USA) and a nuclear counterstain (Gill’s hematoxylin; Thermo Shandon, Pittsburgh, PA, USA). Pre-immune rabbit serum (1000-fold dilution) was applied to adjacent negative control sections.

### *Statistical analysis*

All data were individually expressed as mean ± SD. When statistical analyses were performed, data were compared by one-way ANOVA or Student's t-test, setting statistical significance at $p<0.05$.

# Results

### *Mimecan are mainly expressed in adrenal cortex and medullary mesenchyme.*

In this study, we first examined the distribution of mimecan in adrenal tissues of the C57BL/6 mouse using immunohistochemistry and *in situ* hybridization. As indicated by the results of polyclonal anti-mimecan immunostaining, mimecan expressed mainly in adrenal cortex (**Fig. 1I-L**). This is consistent with results of *in situ* hybridization using fluorescein-labeled mimecan antisense RNA probes (**Fig. 1A-B**). Adrenal medullary cells are chiefly composed of adrenaline- and noradrenaline-releasing chromaffin cells, both expressing catecholamine synthesizing enzymes, such as tyrosine hydroxylase (TH) and dopamine β-hydroxylase (DBH). Adrenaline-releasing cells alone harbor phenylethanolamine-N methyl transferase (PNMT), an enzyme that methylates noradrenaline, converting it to adrenaline. Adrenomedullin (AM) is a hormone that is highly expressed in adrenal medullary mesenchyme. To clarify mimecan expression in adrenal medulla, we performed dual-color *in situ* hybridization of mimecan and PNMT or TH or AM. As a result, neither PNMT (blue) expression in adrenaline-releasing cells of adrenal medulla nor TH (blue) expression in most of adrenal medulla was co-expressed with mimecan (red) (**Fig. 1C-F**). However, AM (blue) and mimecan (red) are co-expressed in the medullary mesenchyme (**Fig. 1G and H**). In conclusion, these results revealed that, in the mouse adrenal gland, mimecan is mainly expressed in the cortex although being also detected in the medulla.

The adrenal cortex is responsible for synthesis of glucocorticoid, which are essential for survival under stress. Given the high-level of adrenocortical mimecan expression demonstrated by our previous and present studies(11, 12), we presumed that mimecan may be involved in regulating functions of the HPA axis during responses to stress.

### *Mimecan expression in adrenal tissue was decreased after acute stress*

We used insulin-induced hypoglycemia in mice as a model to investigate the expression of mimecan after acute stress(18). The test mice were fasted 12h overnight and then given insulin (3 IU/kg body weight) by IP injection. Blood glucose was subsequently measured at various time points. Blood glucose levels were all below 40 mg/dl, showing a successfully induced hypoglycemia state in stressed group (**Table 1**). As anticipated, expression of StAR, which is a marker of stress, was induced by hypoglycemic stress, showing significant upregulation 1 h after insulin dosing and peaking at 6 h (**Fig. 2A**). Interestingly, significant time-dependent downregulation of mimecan expression was observed (**Fig. 2B**). However, blood glucose had normalized 8 h after insulin administration (**Table 2**), implying that reduced mimecan expression constitutes a response to stress induced by hypoglycemia rather than hypoglycemia state. To exclude the possibility that StAR up-regulation and mimecan down-regulation was induced by insulin directly rather than insulin induced hypoglycemia stress, we examined StAR and mimecan mRNA levels after insulin stimulation in the Y1 cell (**Fig. 2C and 2D**). No significant change of StAR and mimecan

mRNA levels was observed 2h and 6h after insulin stimulation. To further verify this result, we established burn trauma stress model in mice as described. In situ hybridization showed that expression levels of StAR mRNA significantly increased in adrenal tissues of mice after scalding (**Fig. 2E**), so this stress model appeared sound. Northern blot showed a significant downregulation of mimecan in adrenal tissue, whereas levels in mouse lung and adipose tissues were unchanged after scalding (**Fig. 2F**). Above results revealed that Mimecan expression in adrenal tissue was significantly decreased after acute stress.

### *Stress-related mimecan downregulation was mediated directly by ACTH rather than ACTH induced glucocorticoid secretion.*

Activation of the HPA axis and the accompanying hormonal response to stress is triggered by a surge of CRH into the hypothalamic-pituitary-portal system. Elevated CRH in portal blood increases ACTH secretion in the pituitary and produces a corresponding rise in adrenal glucocorticoid secretion(19). To determine whether decreased mimecan expression after stress are mediated by increased ACTH secretion, we administrated ACTH to C57BL/6 mice at doses of 0.085 U/g at 2, 4, 6, 8, and 12 h. The animals were then sacrificed at various time points, and their adrenal glands were collected bilaterally at once, using Northern blot to sequentially assess mimecan mRNA expression in adrenal tissues of these mice. The stated levels showed significant time-dependent declines after ACTH dosing (**Fig. 3A**). Compared with controls, expression of mimecan in adrenal tissues was reduced by ~70% at 2 h and ~90% at 6 h post-treatment (**Fig. 3A**), whereas corresponding levels in lung tissue were unchanged (**Fig. 3B**). We also detected mimecan expression after ACTH treatment in primary cultures of mouse adrenal cells (**Fig. 3C**). Similarly, fresh adrenal cellular isolates cultured with 1 μM ACTH for 6 h and 12 h revealed declines in mimecan mRNA levels compared with controls (**Fig. 3C**). Considering the complexity of mice, we again applied this strategy to the Y1 adrenocortical cell line. The cells were treated with $10^{-10}$, $10^{-8}$, and $10^{-6}$ M ACTH for 12 h, assessing mimecan mRNA levels by Northern blot (**Fig. 3D**) and real-time quantitative PCR (**Fig. 3F**). Mimecan expression in Y1 cells was downregulated by ACTH treatment in a dose-dependent manner. Compared with controls, expression of mimecan in the Y1 cell line was reduced by 40% at $10^{-8}$ M and 60% at $10^{-6}$ M after a 12-h ACTH exposure (**Fig. 3D and 3F**); and mimecan mRNA levels declined in a time-dependent manner after 1 μM ACTH treatment, as shown by Northern blot (**Fig. 3E**) and real-time quantitative PCR (**Fig. 3G**).

Because our previous study found that glucocorticoid up-regulates mimecan expression in corticotroph cells(11), We also examined the effects of DEX on mimecan expression in adrenal tissues. In accordance with the results in corticotrophin cells, mRNA levels of mimecan in adrenal tissues of C57BL/6 mice was markedly upregulated in a time-dependent manner after IM injection of DEX (0.05 ug/g body weight), which peaked at 12 h and were sustained for 36 h (**Fig. 4A**). Likewise, mimecan expression in Y-1 cells increased significantly in time- (**Fig. 4B and 4D**) and dose-dependent manners (**Fig. 4C and 4E**) after DEX exposure. Moreover, the DEX-induced increase in Y1 cellular expression of mimecan was abolished by treatment with 1 μM RU486, a GR blocker (**Fig. 4C and 4E**). The results seem contradictory, but it may be explained by that ACTH inhibits mimecan to prevent excessive secretion of glucocorticoid after acute stress because we found mimecan also promote glucocorticoid secretion in **Fig. 5A**. Moreover, the fact

that ACTH lowered mimecan expression and DEX increased its expression during in vivo and in vitro studies clearly indicates that the effects of stress on the downregulation of mimecan expression in adrenal tissues are mediated by ACTH rather than glucocorticoid.

### *Mechanism of inhibited adrenal mimecan expression due to ACTH*

Binding of ACTH to its receptor generally activates the following four signaling pathways: 1) cAMP/PKA/CREB; 2) MEK/ERK; 3) PKC; and 4) JNK. The cAMP/PKA/CREB pathway is responsible for upregulated StAR expression, which is otherwise downregulated by activated MEK/ERK, PKC, or JNK pathways. To investigate those pathways mediating the effects of ACTH on mimecan expression, Y1 cells were separately treated with specific inhibitors of four ACTH signaling pathways (SQ22536 for cAMP, H89 for PKA, PD98059 and U0126 for ERK, GO6983 for PKC, and SP600125 for JNK) for 40 minutes prior to 1 μM ACTH stimulation. As expected, mRNA levels of StAR were significantly upregulated in Y1 cell lines at 6 h and then abolished after treatment with cAMP/PKA inhibitors, H89 (20 μM) or SQ22536 (200 μM) (**Supplementary Fig. 1A, 1B** and **1E**). However, the observed lowering of mimecan mRNA in Y1 cells induced by ACTH was not reversed after treatment with the cAMP/PKA pathway inhibitor, H89 (20 μM) or SQ22536 (200 μM) (Fig 3F, **Supplementary Fig. 2A** and **2B**). Both the PKC inhibitor GO6983 and JNK inhibitor SP600125 did not reversed the observed lowering of mimecan mRNA in Y1 cells induced by ACTH (**Fig 4F**, **Supplementary Fig. 2C** and **2D**) and the stimulation effects of ACTH on StAR (**Supplementary Fig. 1C**, **1D** and **1E**). It is therefore likely that inhibition of mimecan expression in adrenal cells due to ACTH is not mediated by the cAMP/PKA/CREB, PKC, or JNK pathway. However, the inhibitory effects of ACTH on mimecan expression in Y1 cells after 6-h stimulation by 1 μM ACTH was abolished by treatment with the ERK inhibitors, PD98059 (25 μM, 50 μM) and U0126 (10 nM, 20 nM) (**Fig. 4G**). Consequently, ACTH downregulation of mimecan expression in adrenal cells is likely mediated by the ERK signaling pathway.

### *Mimecan stimulates secretion of corticosterone in mouse adrenal cells*

Having shown that mimecan is downregulated by ACTH and that corticosterone increases mimecan expression in adrenal tissues, we further investigated whether mimecan regulates ACTH and corticosterone secretion. C57BL/6 mice received IP injections of mimecan-MBP fusion protein, PBS, or MBP alone at doses of 0.1 μmol/kg body weight. Whole blood was then obtained from retroorbital spaces for ACTH and corticosterone assay (ELISA). Serum corticosterone concentrations were much higher in C57BL/6 mice receiving mimecan-MBP fusion protein at the stated dose than in recipients of PBS or MBP (**Fig. 5A**). Compared with controls, serum corticosterone was significantly elevated at 0.5 h after IP injection of mimecan-MBP fusion protein, reaching a peak at 2 h, maintaining high levels for at least 4 h, and then normalizing at 24 h (**Fig. 5A**). Serum levels of ACTH did not differ significantly among any of these treatment groups (**Fig. 5B**). These data suggest that mimecan-induced corticosterone secretion is not mediated by heightened levels of ACTH. Compared with MBP-treated Y1 cells, the concentration of corticosterone in culture media clearly increased after treatment with mimecan-MBP fusion protein for 24 h, as opposed 8 h at a dose of 7.64 μM (**Fig. 5C**). To determine the mechanism for

corticosterone elevation, expression levels of key genes regulating corticosterone synthesis in adrenal tissues, such as StAR, CYP11A1, CYP11B1 and CYP21, were detected using real-time PCR. Remarkably, expression levels of these genes in the adrenal tissues of mice were substantially downregulated 4 h after IP injection of mimecan-MBP fusion protein (**Fig. 5D-G**). Therefore, the observed mimecan-induced rise in corticosterone concentrations of mouse serum or Y1-cell culture media were probably due to intensified corticosterone secretion by stimulated adrenal cortical cells rather than increased corticosterone synthesis.

### *Mimecan deficiency disturbs stress-free diurnal rhythms of corticosterone secretion, enhancing HPA activation in a mimecan knockout mouse restraint model*

We further generated mimecan knockout mice to delineate the physiologic roles of mimecan(12). In stress-free states, serum corticosterone and ACTH levels (**Fig. 6A and 6B**) and mRNA expression levels of genes involved in corticosterone synthesis (**Supplementary Fig. 3A-D**) were similar for knockout mice and wild-type litter mates. However, the diurnal rhythm of corticosterone secretion in knockout vs wild-type mice was disturbed significantly, as shown by serial determinations of serum corticosterone collected at 8:00, 12:00, 16:00, 20:00, 0:00, and 4:00 hours in an unstressed state (**Fig. 6C**). In wild-type mice, these levels peaked in the evening (20:00 hours) and reached a nadir in the morning, reflecting non-stressful circadian secretion of cortisol (**Fig. 6C**). However, no clear peaks or troughs of serum corticosterone were encountered in counterpart knockout mice, only a flattened pattern (**Fig. 6C**). To explore the responses of mimecan knockout mice to ACTH and glucocorticoid, these mice were received IP injections of ACTH (0.085 IU/g body weight) and IM injections of DEX (0.05 ug/g body weight). Although serum corticosterone levels in knockout and wild-type mice after ACTH stimulation did not differ significantly (**Fig. 6D**), serum corticosterone levels were lower in knockout vs wild-type mice following IM DEX injection for 5h to 32h (**Fig. 6E**), which may due to the absence of corticosterone boosting effects of mimecan in knockout mice. Meanwhile, serum ACTH levels remained comparable in both groups of mice (**Fig. 6F**), and mRNA expression levels of genes encoding corticosterone synthesis enzymes also showed no difference between knockout and wild-type mice after IM DEX injection. (**Supplementary Fig. 3E-H**).

We also investigated whether genetic mimecan deficiency influenced pituitary and adrenal gland function in response to stress. Male knockout mice and wild-type litter mates were restrained for 60 min to inflict physical stress. We collected blood through tail cuts at the time of release and 60 min later, measuring serum corticosterone by ELISA. Restraint of knockout mice for 60 min induced a significantly greater increase in serum corticosterone compared with levels in wild-type litter mates (**Fig. 6G**). Moreover, the observed difference in serum corticosterone concentrations between knockout and wild-type mice was lost 60 min after release (**Fig. 6G**). These findings indicate a striking excess of the response to stress in knockout mice.

Table 1
Blood glucose measurement during hypoglycemic stress.

| Group | Mean value of blood glucose at 0h(mmol/L) | Mean value of blood glucose at sacrifice(mmol/L) |
|---|---|---|
| control | / | 9.35 ± 0.88 |
| case-1 h | 4.64 ± 0.78 | 1.78 ± 0.34 |
| case-2 h | 4.75 ± 0.49 | 1.46 ± 0.37 |
| case-4 h | 4.87 ± 0.46 | 1.77 ± 0.48 |
| case-6 h | 5.63 ± 0.40 | 3.67 ± 0.51 |
| case-8 h | 5.36 ± 0.55 | 5.23 ± 0.62 |
| case-12 h | 4.36 ± 0.72 | 6.20 ± 0.48 |

# Discussion

Although implicated in many biologic processes, the physiologic functions of mimecan remain elusive. It is most extensively researched in keratocytes of the bovine cornea, where it likely helps maintain matrix homeostasis(20, 21). Apart from its important roles in the regulating construction of extracellular matrix, the expression deficiency or down regulation of mimecan has been indicated in several kinds of tumors(22–24). A prior study of ours aimed at lung cancer has shown the considerable promise of mimecan as a biomarker, helping to distinguish non-small-cell from small-cell lung cancer pathologic types(25). Expression of mimecan mRNA and protein were also observed in the human anterior pituitary glands. Luciferase reporter analysis and electrophoretic mobility shift assays indicate that pituitary transcription factor-1 (Pit-1), expressed solely in the pituitary, is capable of activating the human mimecan promoter via Pit-1 response-element sites(18). Most recently, we have discovered that as a newly recognized adipokine, mimecan can inhibit food intake by inducing IL-1β and IL-6 expression in the hypothalamus(10). This body of evidence attests to the diverse actions of mimecan in many physiologic and pathologic processes.

According to the present findings, mimecan is primarily expressed in adrenal cortex. We found that its expression in adrenal tissue was significantly downregulated under stress in our mouse model, signifying a role in stress response. We also determined that expression of mimecan in adrenal cells may be downregulated by ACTH and upregulated by DEX. Although both dramatic increases in levels of secreted ACTH and corticosterone were apparent in mice after stress, the data herein clearly illustrate that stress-induced downregulation of mimecan in adrenal tissues is mediated by ACTH, rather than corticosterone.

Cortisol is the terminal effector of the HPA axis, and cortisol secretion is stimulated as a result of HPA activation in response to acute stress. It is generally acknowledged that cortisol secreted by adrenal cortex is directly tied to pituitary ACTH release. In recent years, however, there is mounting evidence that

many adrenomedullary secretory products, such as adrenomedullin, catecholamines, 5-HT, neuropeptides, and growth factors, take part in regulating adrenocortical steroidogenesis via non-ACTH-dependent pathways(26–28). Furthermore, cytokines produced by adrenal cells themselves are capable of directly influencing adrenocortical function. They may stimulate steroidogenesis (similar to IL-1, IL-2, and IL-6) or exert regulatory effects on adrenal growth (as does TNFα or interferon-γ)(29–32). It is a proven fact that cortisol release is self-regulated through a CNS negative feedback loop involving receptors in pituitary, PVN, and other brain structures(33). However, little is known of similar synthesis/secretion autoregulation via intra-adrenal mechanisms.

In the present study, based on *in vivo* and *in vitro* studies, we found that mimecan stimulates corticosterone secretion from adrenal tissues in a short time response, yet there were no *in vivo* effects on serum levels of ACTH. Additionally, mimecan expression may be upregulated by corticosterone, as shown by DEX administration studies (*in vitro* and *in vivo*), and this effect vanished after treating Y-1 adrenal cells with RU486 (a GR inhibitor), which is in accord with our previous results that mimecan expressed in pituitary corticotrophin cells is increased by glucocorticoid and that its upregulation may be mediated through classic GR pathways(11). Our findings therefore suggest that under basal conditions, mimecan may stimulate glucocorticoid release from adrenal cells as a means of positive feedback (Fig. 6H), although this premise is still tentative. Collectively, our data support the concept of ACTH-independent glucocorticoid regulation, permitting self-regulation of synthesis and secretion within the adrenal gland owing to upregulation of intra-adrenal mimecan expression.

Another interesting facet of this study was that mimecan deficiency in mice fosters disturbances in diurnal rhythms of corticosterone secretion and stronger responses to restraint stress, despite the similar serum ACTH and corticosterone concentrations seen in wild-type and mimecan knockout mice under basal conditions. Consequently, it is tempting to presume that mimecan plays a vital intra-adrenal role, helping to maintain glucocorticoid homeostasis in mice after acute stress. In basal states of moderate-level ACTH release, glucocorticoid promotes mimecan expression in adrenal tissues through GRs, in turn prompting secretion of glucocorticoid to sustain appropriate levels. Thus, a positive intra-adrenal feedback loop seems to be at work. However, stress-related increases in ACTH release due to HPA axis over-activation will then culminate in downregulation of intra-adrenal mimecan expression, attenuating its effects on glucocorticoid secretion and avoiding glucocorticoid excess. In mimecan knockout mice, this negative feedback effect during acute stress is lost, explaining their comparatively stronger responses to stress.

In conclusion, we have demonstrated for the first time the critical role that mimecan likely plays in regulating the HPA axis. In the absence of mimecan effects, we observed disturbed circadian rhythms of corticosterone secretion in C57BL/6 mice and abnormal secretion of corticosterone in response to stress or exogenous steroid stimulation. Although ACTH may inhibit mimecan expression in adrenal tissues, any mechanisms of mimecan control are still unknown. Future studies investigating the impact of mimecan on corticosterone secretion are clearly warranted.

# Declarations

### Ethics approval and consent to participate

The animal study was performed in accordance with the approved protocol by the Animal Care and Use Committee in the Ninth Hospital Affiliated to Shanghai Jiaotong University School of Medicine.

### Consent for publication

Not applicable.

### Availability of data and materials

The datasets used and/or analysed during the current study are available from the corresponding author on reasonable request.

### Competing interests

The authors declare that the research was conducted in the absence of any commercial or financial relationships that could be construed as a potential conflict of interest.


### Funding

The work was supported in part by National Key R&D Program of China (HS, No. 2017YFC1001801), National Natural Science Foundation of China (BS, No. 81101444, HS, No. 81770786, 81661168016, 81430019, 81370888; YR, 81000321; SZ, No. 31571296; CZ, 81472177).


### Author's contribution

HS, BS and YR conceived and designed the project. BS, YR, XL, CZ and QZ contribute to the project management. BS and YR conducted most of the experiments. BS, XL, PL and JM designed and performed animal experiments. YR and FS designed and performed cell experiments. HC purified the MBP-mimecan protein. QZ, BS and YR took part in the statistical analysis. QZ and HS wrote the manuscript. BS, YR, QZ and HS reviewed, edited and revised the manuscript. All co-authors read and gave input to help improve the manuscript.


### Acknowledgements

Not applicable.


# References


1. Chrousos GP, Gold PW. The concepts of stress and stress system disorders. Overview of physical and behavioral homeostasis. JAMA. 1992;267(9):1244-52.

2. Lightman SL. The neuroendocrinology of stress: a never ending story. J Neuroendocrinol. 2008;20(6):880-4.
3. Myers B, McKlveen JM, Herman JP. Neural Regulation of the Stress Response: The Many Faces of Feedback. Cell Mol Neurobiol. 2012.
4. Keck ME, Holsboer F. Hyperactivity of CRH neuronal circuits as a target for therapeutic interventions in affective disorders. Peptides. 2001;22(5):835-44.
5. Claes SJ. CRH, stress, and major depression: A psychobiological interplay. Vitam Horm. 2004;69:117-50.
6. Bentz H, Nathan RM, Rosen DM, Armstrong RM, Thompson AY, Segarini PR, et al. Purification and Characterization of a Unique Osteoinductive Factor from Bovine Bone. Journal of Biological Chemistry. 1989;264(34):20805-10.
7. Deckx S, Heymans S, Papageorgiou AP. The diverse functions of osteoglycin: a deceitful dwarf, or a master regulator of disease? Faseb J. 2016;30(8):2651-61.
8. Tasheva ES, Corpuz LM, Funderburgh JL, Conrad GW. Differential splicing and alternative polyadenylation generate multiple mimecan mRNA transcripts. J Biol Chem. 1997;272(51):32551-6.
9. Hu RM, Han ZG, Song HD, Peng YD, Huang QH, Ren SX, et al. Gene expression profiling in the human hypothalamus-pituitary-adrenal axis and full-length cDNA cloning. Proc Natl Acad Sci U S A. 2000;97(17):9543-8.
10. Cao HM, Ye XP, Ma JH, Jiang H, Li SX, Li RY, et al. Mimecan, a Hormone Abundantly Expressed in Adipose Tissue, Reduced Food Intake Independently of Leptin Signaling. Ebiomedicine. 2015;2(11):1718-24.
11. Ma QY, Zuo CL, Ma JH, Zhang XN, Ru Y, Li P, et al. Glucocorticoid up-regulates mimecan expression in corticotroph cells. Mol Cell Endocrinol. 2010;321(2):239-44.
12. Ma QY, Zhang XN, Jiang H, Wang ZQ, Zhang HJ, Xue LQ, et al. Mimecan in pituitary corticotroph cells may regulate ACTH secretion and the HPAA. Molecular and Cellular Endocrinology. 2011;341(1-2):71-7.
13. Park MJ, Yoo SW, Choe BS, Dantzer R, Freund GG. Acute hypoglycemia causes depressive-like behaviors in mice. Metabolism. 2012;61(2):229-36.
14. Qiao L, Lu SL, Dong JY, Song F. Abnormal regulation of neo-vascularisation in deep partial thickness scalds in rats with diabetes mellitus. Burns. 2011;37(6):1015-22.
15. Yasumura Y, Buonassisi V, Sato G. Clonal analysis of differentiated function in animal cell cultures. I. Possible correlated maintenance of differentiated function and the diploid karyotype. Cancer Res. 1966;26(3):529-35.
16. Mao W, Huang X, Wang L, Zhang Z, Liu M, Li Y, et al. Circular RNA hsa_circ_0068871 regulates FGFR3 expression and activates STAT3 by targeting miR-181a-5p to promote bladder cancer progression. J Exp Clin Cancer Res. 2019;38(1):169.

17. Hu SM, Li F, Yu HM, Li RY, Ma QY, Ye TJ, et al. The mimecan gene expressed in human pituitary and regulated by pituitary transcription factor-1 as a marker for diagnosing pituitary tumors. J Clin Endocrinol Metab. 2005;90(12):6657-64.
18. Szilamer F, Edina Z, Bernadett P, Zsuzsanna S, Kovacs KJ. Differential regulation of hypothalamic neuropeptide Y hnRNA and mRNA during psychological stress and insulin-induced hypoglycemia. Molecular and Cellular Endocrinology. 2010;321(2):138-45.
19. Mascarenhas DD, Elayadi A, Singh BK, Prasai A, Hegde SD, Herndon DN, et al. Nephrilin peptide modulates a neuroimmune stress response in rodent models of burn trauma and sepsis. Int J Burns Trauma. 2013;3(4):190-200.
20. Owens MJ, Nemeroff CB. Physiology and Pharmacology of Corticotropin-Releasing Factor. Pharmacol Rev. 1991;43(4):425-73.
21. Funderburgh JL, Corpuz LM, Roth MR, Funderburgh ML, Tasheva ES, Conrad GW. Mimecan, the 25-kDa corneal keratan sulfate proteoglycan, is a product of the gene producing osteoglycin. Journal of Biological Chemistry. 1997;272(44):28089-95.
22. Dunlevy JR, Beales MP, Berryhill BL, Cornuet PK, Hassell JR. Expression of the keratan sulfate proteoglycans lumican, keratocan and osteoglycin/mimecan during chick corneal development. Exp Eye Res. 2000;70(3):349-62.
23. Li L, Zhang ZW, Wang CY, Miao L, Zhang JP, Wang JS, et al. Quantitative Proteomics Approach to Screening of Potential Diagnostic and Therapeutic Targets for Laryngeal Carcinoma. Plos One. 2014;9(2).
24. Wang YH, Ma Y, Lue BJ, Xu E, Huang Q, Lai M. Differential expression of mimecan and thioredoxin domain-containing protein 5 in colorectal adenoma and cancer: A proteomic study. Exp Biol Med. 2007;232(9):1152-9.
25. Rower C, Ziems B, Radtke A, Schmitt O, Reimer T, Koy C, et al. Toponostics of invasive ductal breast carcinoma: combination of spatial protein expression imaging and quantitative proteome signature analysis. Int J Clin Exp Patho. 2011;4(5):454-67.
26. Zheng CX, Zhao SX, Wang P, Yu HM, Wang CF, Han B, et al. Different expression of mimecan as a marker for differential diagnosis between NSCLC and SCLC. Oncol Rep. 2009;22(5):1057-61.
27. Bornstein SR, Chrousos GP. Clinical review 104: Adrenocorticotropin (ACTH)- and non-ACTH-mediated regulation of the adrenal cortex: neural and immune inputs. J Clin Endocrinol Metab. 1999;84(5):1729-36.
28. Ehrhart-Bornstein M, Hinson JP, Bornstein SR, Scherbaum WA, Vinson GP. Intraadrenal interactions in the regulation of adrenocortical steroidogenesis. Endocr Rev. 1998;19(2):101-43.
29. Zacharowski K, Zacharowski PA, Koch A, Baban A, Tran N, Berkels R, et al. Toll-like receptor 4 plays a crucial role in the immune-adrenal response to systemic inflammatory response syndrome. Proc Natl Acad Sci U S A. 2006;103(16):6392-7.
30. Gwosdow AR, O'Connell NA, Spencer JA, Kumar MS, Agarwal RK, Bode HH, et al. Interleukin-1-induced corticosterone release occurs by an adrenergic mechanism from rat adrenal gland. Am J

Physiol. 1992;263(3 Pt 1):E461-6.

31. Tominaga T, Fukata J, Naito Y, Usui T, Murakami N, Fukushima M, et al. Prostaglandin-dependent in vitro stimulation of adrenocortical steroidogenesis by interleukins. Endocrinology. 1991;128(1):526-31.
32. Ilvesmaki V, Jaattela M, Saksela E, Voutilainen R. Tumor necrosis factor-alpha and interferon-gamma inhibit insulin-like growth factor II gene expression in human fetal adrenal cell cultures. Mol Cell Endocrinol. 1993;91(1-2):59-65.
33. Voutilainen R, Ilvesmaki V, Ariel I, Rachmilewitz J, de Groot N, Hochberg A. Parallel regulation of parentally imprinted H19 and insulin-like growth factor-II genes in cultured human fetal adrenal cells. Endocrinology. 1994;134(5):2051-6.

# Figures

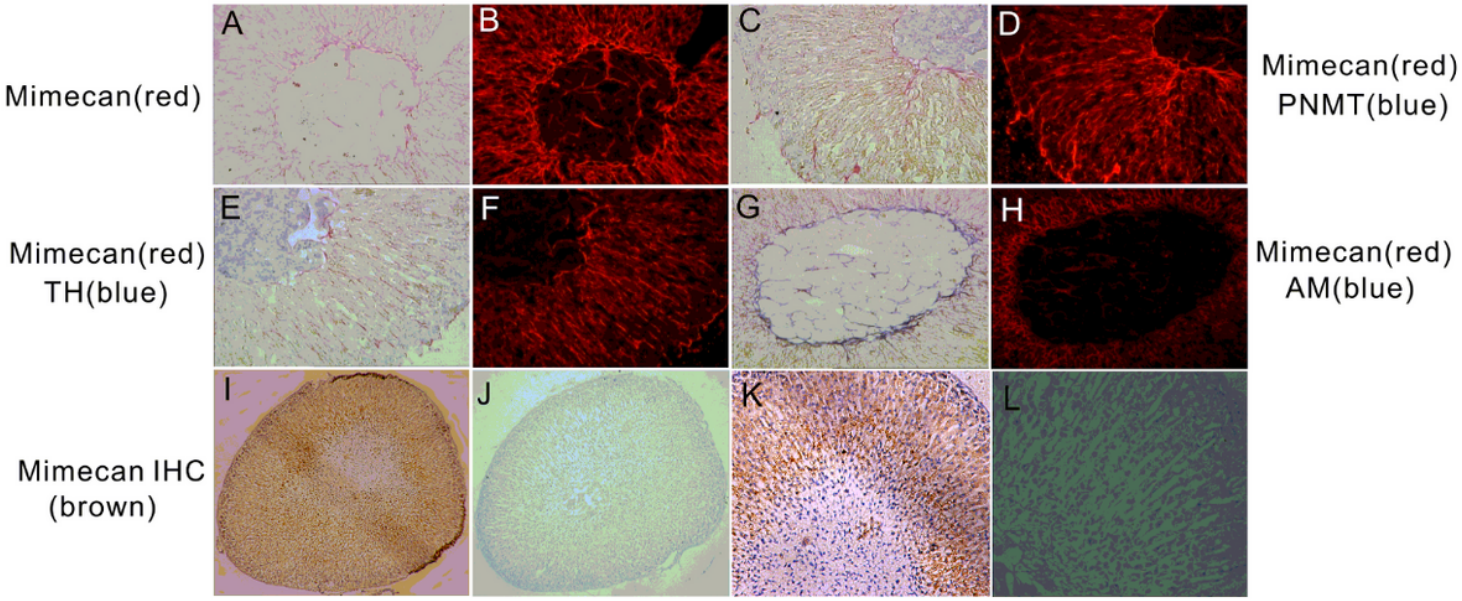


**Figure 1**

Localization of mimecan expression in mouse adrenal glands using in situ hybridization and immunohistochemistry. (A) Positive staining (red) of sections of adrenal gland hybridized with DIG-labeled mimecan antisense probes primarily appeared in the adrenal cortex and some of the medullary mesenchyme (image obtained under visible light at 10× magnification). (B) Field shown is the same as (A) under fluorescent light. (C) Sections of adrenal gland hybridized with fluorescein-labeled mimecan and DIG-labeled PNMT antisense probes, confirming mimecan expression (red) primarily within adrenal cortex while PNMT (blue) was in medulla; no co-expression was observed (image obtained under visible light at 10× magnification). (D) Field shown is the same as (C) under fluorescent light. (E) Sections of adrenal gland hybridized with fluorescein-labeled mimecan and DIG-labeled TH antisense probes,

confirming mimecan expression (red) primarily within adrenal cortex while TH (blue) was in medulla; no co-expression was observed (image obtained under visible light at 10× magnification). (F) Field shown is the same as (E) under fluorescent light. (G) Sections of adrenal gland hybridized with fluorescein-labeled mimecan and DIG-labeled ADREAM antisense probes, confirming mimecan expression (red) primarily within adrenal cortex; mimecan and ADREAM co-expression was observed in the medulla (image obtained under visible light at 10× magnification). (H) Field shown is the same as (G) under fluorescent light. (I)Sections of formalin-fixed, paraffin-embedded adrenal gland immunostained with rabbit anti-human mimecan antibody and anti-rabbit IgG antibody. Positive (brown) staining was found primarily in adrenal cortex. (J) Negative control of (I) with pre-immune rabbit serum used in lieu of mimecan antibody. (K-L) Higher magnifications of (I) and (J).

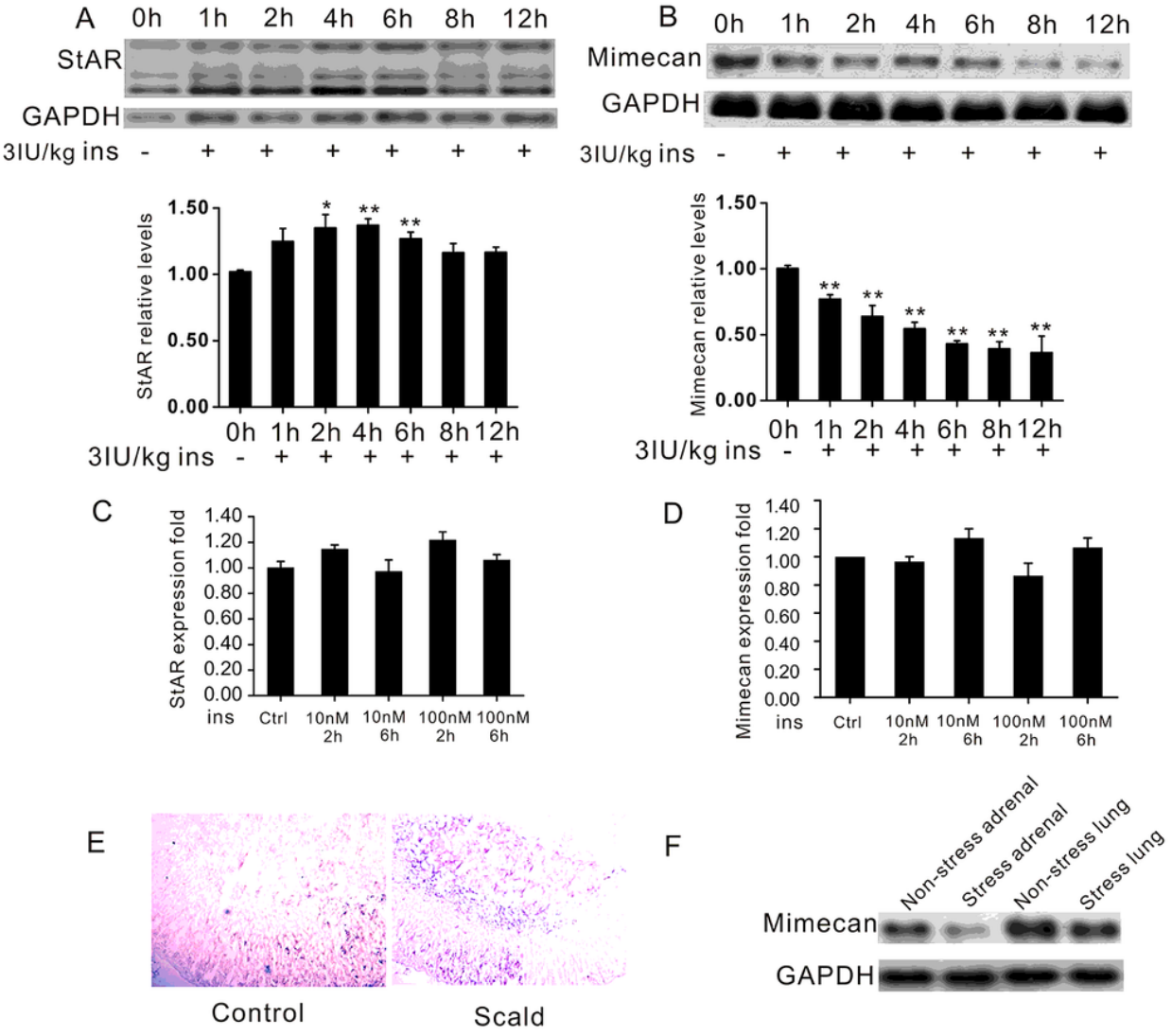


## Figure 2

Downregulation of mimecan expression in adrenal glands during stress. (A) Northern blot and quantified results confirming the expected increase of StAR gene expression in C57BL/6 male mice subjected to hypoglycemic stress and time-dependent reduction of mimecan gene expression in adrenal gland of C57BL/6 male mice subjected to hypoglycemic stress (10 mice for each time point). Mice were fasted 12

h and injected with insulin (3 IU/kg). (C, D) StAR and Mimecan mRNA levels in Y1 cell after insulin treatment by Realtime PCR. (E) Sections of adrenal glands hybridized with fluorescein-labeled StAR antisense probes. Positive signals (blue) was significantly increased compared with controls (image obtained under visible light at 10× magnification). (F) Analysis of mimecan expression by Northern blot in scalded C57BL/6 male mice (15 mice per group), showing pronounced downregulation of mimecan mRNA in adrenal glands specifically and no change in lung tissues. Data information: *p<0.05, **p<0.01, ***p<0.001 for stress treatment vs control.

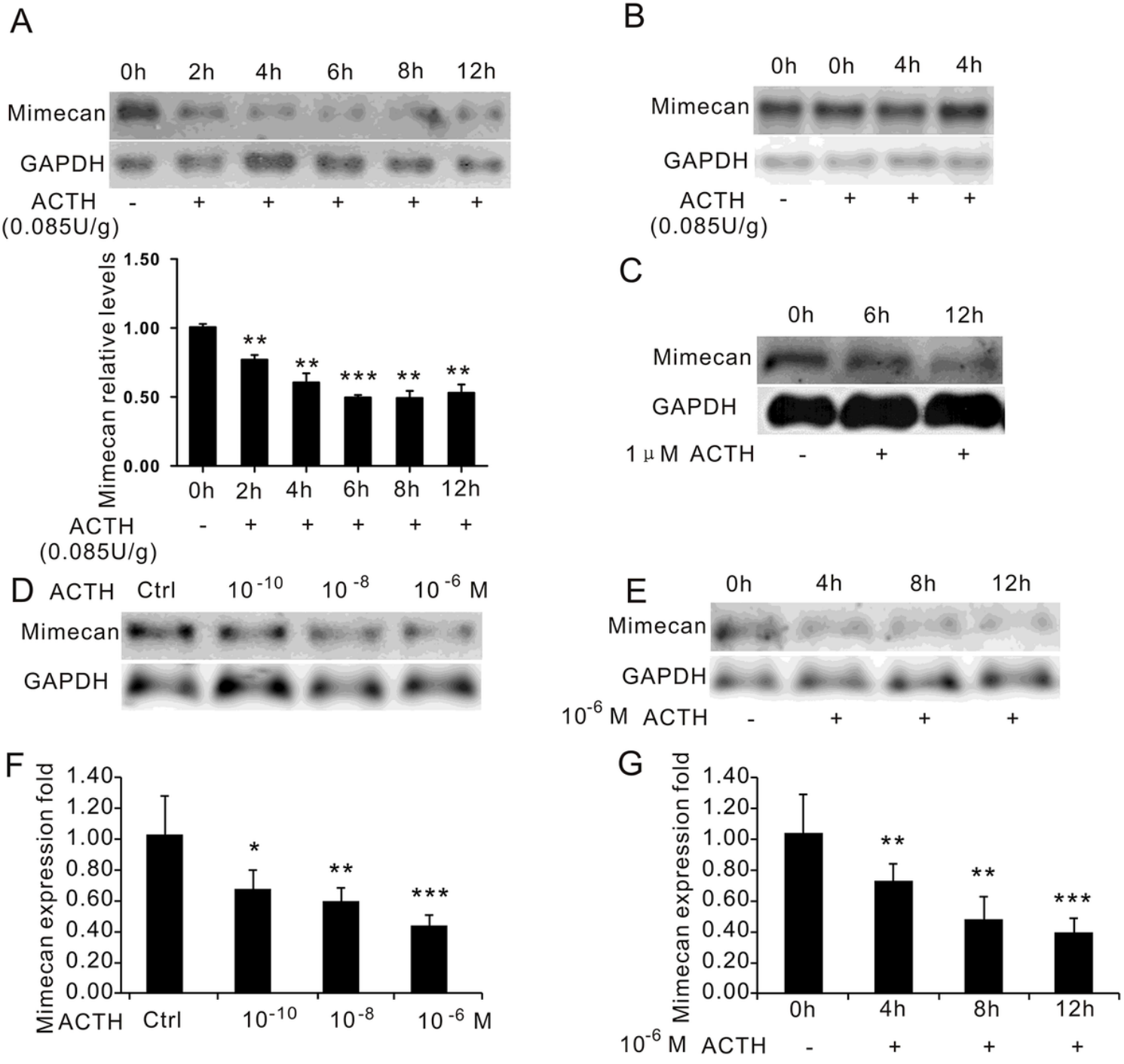


**Figure 3**

Inhibition of mimecan expression in time- and dose-dependent manners by ACTH administration. (A) Mimecan mRNA expression was detected by Northern blot in adrenal glands of C57BL/6 male mice after intraperitoneal injection of ACTH (0.085 U/g; 12 mice per group for each time point). Note the significant time-dependent decline. (B) No change in lung tissue expression of mimecan was observed after ACTH dosing. (C) Northern blot showing that expression of mimecan in primary adrenal cells decreased at various time points after administration of 1 μM ACTH (6 or 7 mice for each time point). (D, E) Northern blot showing ACTH-induced dose-dependent (D) and time-dependent (E) inhibition of mimecan mRNA in Y-1 cells. ACTH dose in (E) was 10-6 M. Y-1 cells were serum-deprived overnight before adding ACTH. (F, G) Realtime PCR showing ACTH-induced dose-dependent (F) and time-dependent (G) inhibition of mimecan mRNA in Y-1 cells. Relative mimecan mRNA levels were normalized to GAPDH mRNA expression and compared with untreated controls. Data information: *p<0.05, **p<0.01, ***p<0.001 for ACTH treatment vs control.

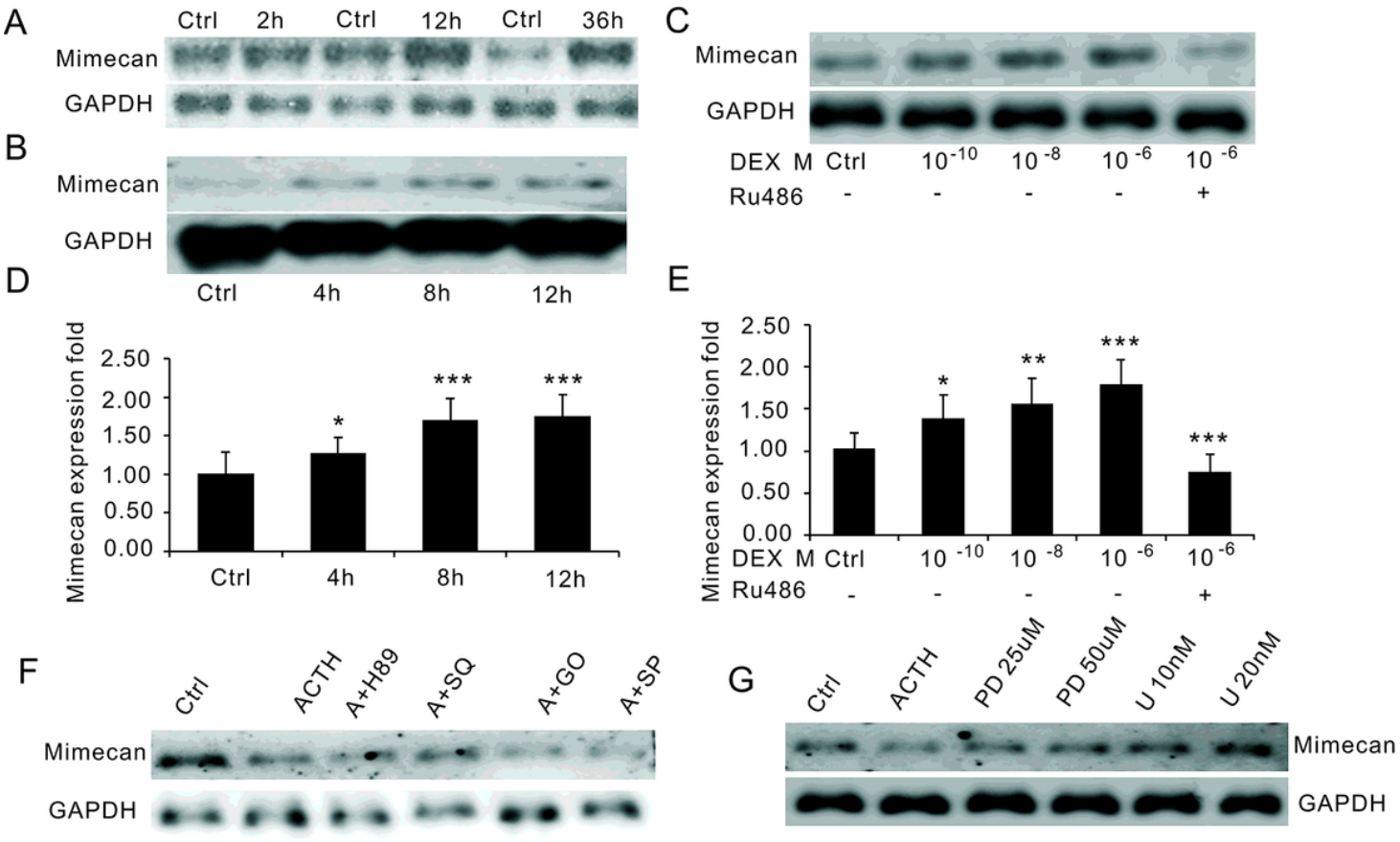


## Figure 4

DEX increases mimecan expression in mice and Y-1 cells. Northern blot reflecting time-dependent increase in mimecan mRNA expression in the adrenal tissues of the C57BL/6 male mice after intramuscular injection of DEX (0.05 μg/g; 10 mice per group for each time point). (B) The time-dependent increase in mimecan mRNA in Y-1 cells after DEX treatment (10−6 M), analyzed using Northern blot. Y-1 cells were serum-deprived overnight before adding DEX or DEX + RU486. (C) The dose-dependent increase in mimecan mRNA in Y-1 cells after DEX treatment was abolished by 1 μM RU486, analyzed using Northern blot. (D, E) mRNA levels in (B) and (C) were determined using quantitative real-

time PCR. Relative mimecan mRNA levels were normalized to GAPDH mRNA expression and compared with untreated controls. (F) ACTH-induced suppression of mimecan expression cannot be attributed to PKA, cAMP, PKC, or JNK signaling. (G) The inhibitory effect of ACTH was abolished by the ERK pathway inhibitors PD98059 and U0126, which rescued mimecan expression in a dose-dependent manner. H89: inhibitor of the PKA pathway; SQ: SQ22536, inhibitor of the cAMP pathway; G0: G06983, inhibitor of the PKC pathway; SP: SP600125, inhibitor of the JNK pathway; PD: PD98059, inhibitor of the ERK pathway; U: U0126, inhibitor of the ERK pathway. Y-1 cells were serum-deprived overnight prior to adding inhibitors. Mimecan gene expression in Y-1 cells was analyzed by Northern blot. The relative mimecan mRNA levels were normalized to GAPDH mRNA expression. Data information: *p<0.05, **p<0.01, ***p<0.001 for DEX treatment vs control.

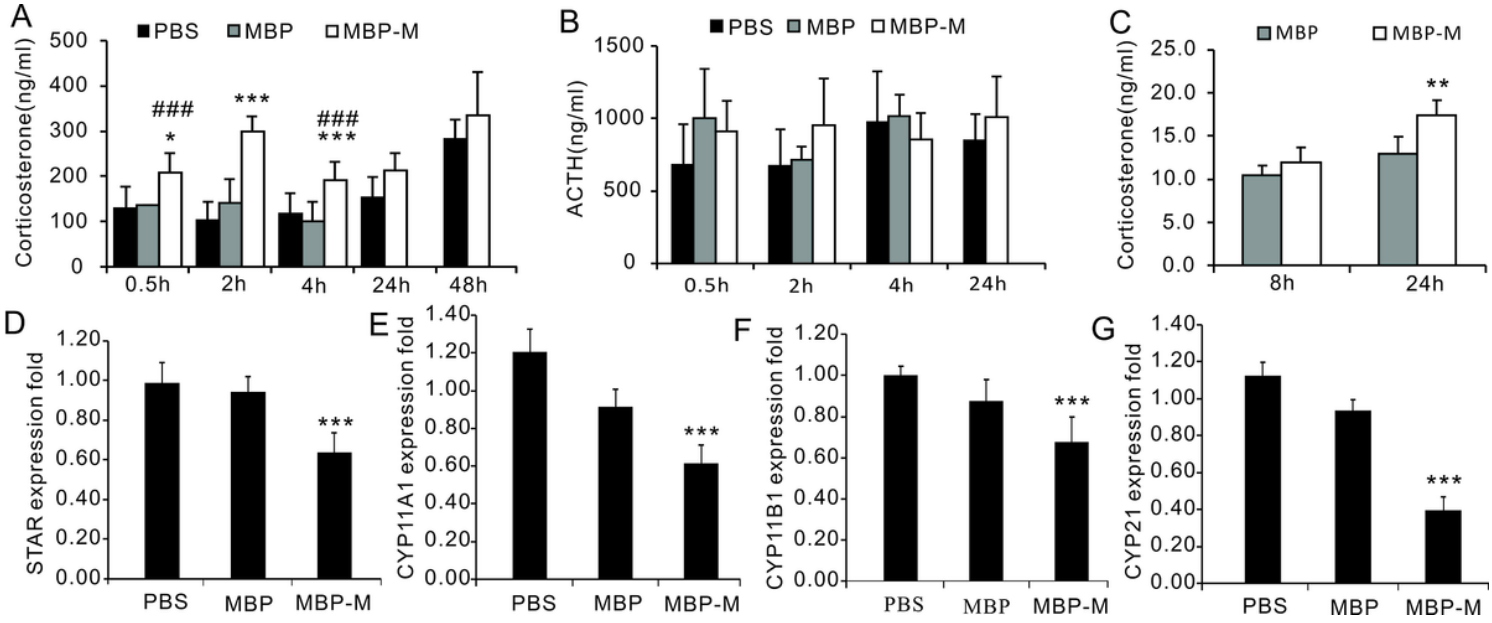


## Figure 5

Mimecan increases corticosterone concentrations in vivo and in vitro with no effect on corticosterone synthesis. (A) Intraperitoneal injection of recombinant mimecan-MBP (vs. MBP and PBS controls) increases serum concentration of corticosterone, normalized 24 h after injection (n=8 per group) in three independent experiments. ***p<0.001 for mimecan-MBP vs MBP treatment, ### p<0.001 for mimecan-MBP treatment at 0.5 h or 4 h vs 2 h. (B) Serum ACTH level was unaffected by intraperitoneal injection of recombinant mimecan-MBP. Serum corticosterone and ACTH were measured using ELISA (8 mice per group). C57BL/6 mice received intraperitoneal injections of recombinant mimecan-MBP (0.1 μmol/kg), MBP (0.1 μmol/kg), or PBS equivalent (controls). (C) Recombinant mimecan-MBP increases corticosterone concentration in culture supernatant of Y1 cells after 24-h treatment at 7.64 μM compared with MBP in three independent experiments. (D-G) mRNA levels of key genes regulating corticosterone synthesis in adrenal tissues declined after intraperitoneal injection of recombinant mimecan-MBP (0.1 μmol/kg) vs MBP or PBS control (8 mice per group). Data information: In (B-G), **p<0.01, ***p<0.001 for mimecan-MBP vs MBP treatment.

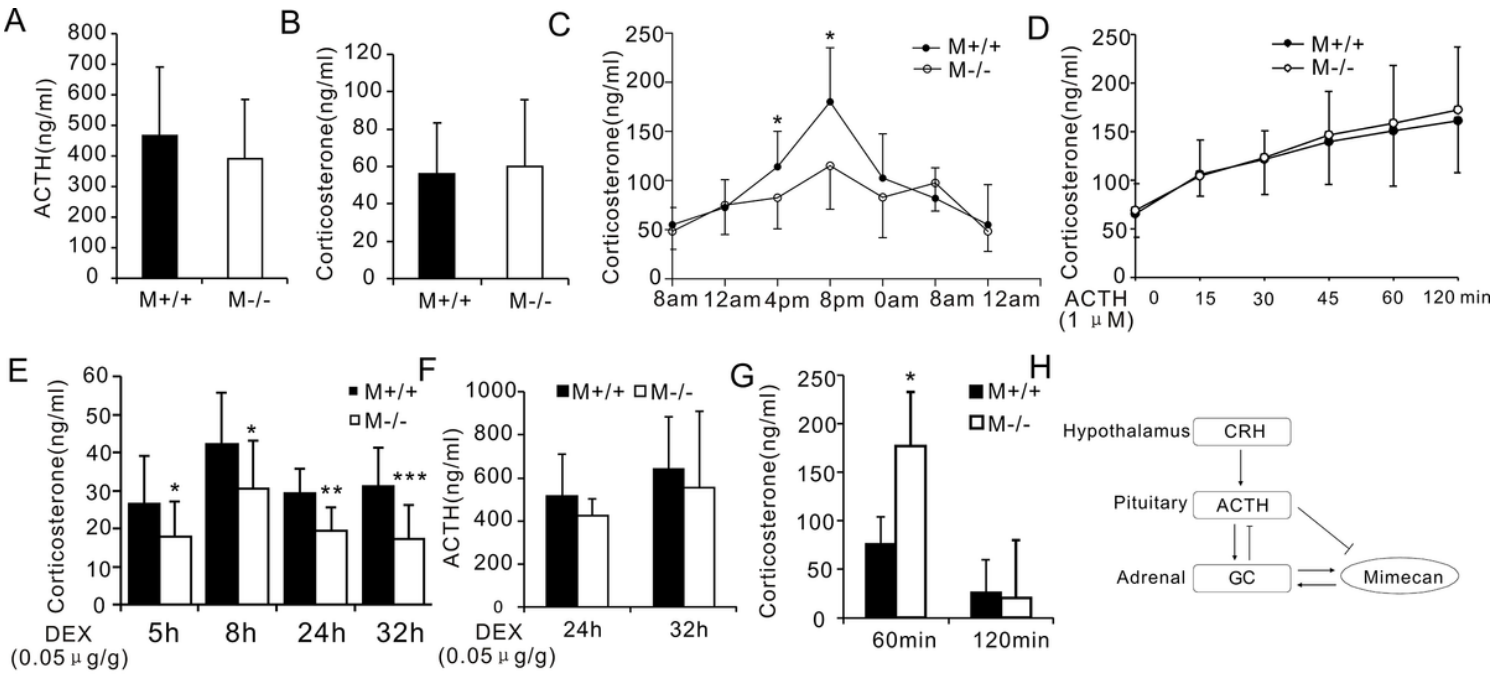


**Figure 6**

Disturbed stress-free diurnal rhythm of corticosterone secretion and hyperactivated stress response in mimecan-deficient mice. (A-B) No difference in serum corticosterone and plasma ACTH levels of wild-type (WT) and mim-/- knockout mice, determined using ELISA (10 mice per group). (C) Significant disturbance of diurnal corticosterone secretion was observed in non-stressed mim-/- mice. Secretion levels lacked the typical peaks and troughs seen with WT mice (n=20 per group). (D) No difference in serum corticosterone levels of wild-type (WT) and mim-/- knockout mice after 1 μM ACTH stimulation. (E) The response to DEX suppression test in mim-/- mice surpasses that of WT mice. Serum corticosterone level was determined using ELISA 5-32 h after intramuscular injection of 0.05 ug/g DEX (21 mim-/- mice and 15 WT mice). (F) Similar serum ACTH levels in mim-/- and WT mice were observed 24-32 h after intramuscular injection of DEX (21 mim-/- mice and 15 WT mice). (G) A marked increased in serum corticosterone levels of mim-/- vs WT male mice was observed after 1 h of restraint and lost 1 h after release (5 mice per group). Data information: *p<0.05 for mim-/- vs WT mice. (H) A graph showing the role of mimecan in HPA axis.

# Supplementary Files

This is a list of supplementary files associated with this preprint. Click to download.

- SupplementaryFig.docx
- FigureS3.tif
- FigureS2.tif
- figureS1.tif
- TableS1.docx